Molecular Cancer

RESEARCH

Open Access

Modulating lipid metabolism by nanoparticles (NPs)-mediated ACSL3 silencing to inhibit hepatocellular carcinoma growth and metastasis

Linzhuo Huang[1,2,3†], Rui Xu[1,2,3†], Siyu Chen[4†], Chunhao Lin[1,2,3], Wende Li[4], Senlin Li[1,5], Phei Er Saw[1,2,3], Lei Zhang[1,5*] and Xiaoding Xu[1,2,3*]

Abstract

Abnormal lipid metabolism plays an important role in the development and progression of almost all cancer types, especially hepatocellular carcinoma (HCC) as the liver is the central organ for lipid storage and metabolism. However, the underlying mechanisms are complex and have not been completely elucidated. By analyzing the proteomic sequencing and single cell RNA-sequencing (scRNA-seq) results of HCC patients, we herein reveal that acyl-CoA synthase long chain family member 3 (ACSL3) is predominately expressed in HCC cells and high ACSL3 expression is positively correlated with abnormal lipid metabolism and predicts the poor prognosis of HCC patients. Mechanically, ACSL3 could promote the synthesis of 1-palmitoyl-2-oleoyl-*sn*-glycero-3-phosphocholine (POPC), which could activate peroxisome proliferator-activated receptor α (PPARα) pathway and enhance the transcription of downstream lipid metabolism-associated genes, thereby promoting HCC growth and metastasis via accelerating lipid catabolism and anabolism. Considering the lack of specific inhibitor for ACSL3, we further develop an endosomal pH-responsive nanoparticle (NP) platform for systemic delivery of ACSL3 siRNA (siACSL3) and demonstrate its ability to inhibit HCC tumor growth and metastasis. Our findings indicate that ACSL3 could be used to predict the prognosis of HCC patients and NPs-mediated ACSL3 silencing could be a promising strategy for effective HCC therapy.

Keywords Lipid metabolism, ACSL3, Nanoparticles, siRNA delivery, Cancer therapy

†Linzhuo Huang, Rui Xu and Siyu Chen have contributed equally to this work.

*Correspondence:
Lei Zhang
zhangl9@mail.sysu.edu.cn
Xiaoding Xu
xuxiaod5@mail.sysu.edu.cn
[1]Guangdong Provincial Key Laboratory of Malignant Tumor Epigenetics and Gene Regulation, Guangdong-Hong Kong Joint Laboratory for RNA Medicine, Medical Research Center, Sun Yat-Sen Memorial Hospital, Sun Yat-Sen University, Guangzhou 510120, P. R. China
[2]Guangzhou Key Laboratory of Medical Nanomaterials, Sun Yat-Sen Memorial Hospital, Sun Yat-Sen University, Guangzhou 510120, P. R. China
[3]Nanhai Translational Innovation Center of Precision Immunology, Sun Yat-Sen Memorial Hospital, Foshan 528200, P. R. China
[4]Guangdong Laboratory Animals Monitoring Institute, Guangzhou 510663, P. R. China
[5]Department of Hepatobiliary Surgery, Sun Yat-Sen Memorial Hospital, Sun Yat-Sen University, Guangzhou 510120, P. R. China

Introduction

Hepatocellular carcinoma (HCC) is one of the most common malignancies and the third leading cause of cancer-related mortalities worldwide [1, 2]. In the past decade, although a great achievement has been made in HCC diagnosis and treatment, the prognosis of HCC patients is still far from expected due to the high probability of recurrence and metastasis. Clinical observations have shown that the 5-year overall survival rate of metastatic HCC patients is less than 12% because of the difficulty in surgical resection and frequently encountered resistance to other therapeutic modalities (e.g., chemotherapy and targeted therapy) [3–5]. In recent years, accumulating evidences have revealed that abnormal metabolism such as altered glucose metabolism from oxidative phosphorylation to aerobic glycolysis significantly contributes to cancer metastasis [6–10]. Therefore, uncovering the key factors regulating abnormal metabolism would have a broad range of implications from the understanding of pathogenic mechanisms to development of new therapeutic targets for effective cancer therapy.

As a hallmark of cancer, abnormal metabolism involves the altered glucose, amino acid, and lipid metabolism and has been observed in almost all cancer types [11–13]. In particular, abnormal lipid metabolism plays a crucial role in the development and progression of HCC as the liver is the central organ for lipid storage and metabolism [8, 14–16]. It has been demonstrated that abnormal lipid metabolism such as increased de novo synthesis of fatty acids and enhanced fatty acid oxidation (FAO) could not only provide more nutrients for the survival, proliferation, and distant metastasis of tumor cells [8, 9], but also supply metabolic intermediates for cellular signal transduction and formation of cell structures [17–19]. Therefore, modulating lipid metabolism could be a promising strategy for effective HCC therapy. In the past decade, various animal models such as high fat diet (HFD)-induced tumor-bearing mouse model have been used to evaluate the influence of abnormal lipid metabolism on cancer progression (e.g., therapeutic resistance and metastasis), and several lipid metabolism-associated factors such as sterol regulatory element-binding protein 1 (SREBP-1) and acetyl-CoA carboxylase (ACC) have been uncovered as new therapeutic targets [20–24]. Nevertheless, the contribution of abnormal lipid metabolism to cancer development and progression remains largely unknown and much more efforts are still required to elucidate the underlying mechanisms. In addition, because of the inherent heterogeneity and complexity of tumor tissues, the use of animal models may not acquire the full spectrum of lipid metabolism in cancer patients [25, 26]. To overcome this limitation, recent advances have focused on the direct analysis of clinical tumor samples by high-throughput sequencing technology. This innovative strategy could not only gain a comprehensive view of the tumor genomic landscape, but also provide broader coverage, higher accuracy, and more clinically relevant insights into the key factors regulating cancer development and progression [27–29].

To extensively explore the influence of abnormal lipid metabolism on HCC metastasis, we herein examine the proteomic expression profiles of matched primary and lung metastatic tumors of HCC patients, and reveal that acyl-CoA synthase long chain family member 3 (ACSL3) is abnormally up-regulated in metastatic tumors of HCC patients. Further analyzing the single cell RNA-sequencing (scRNA-seq) results of HCC patients shows that ACSL3 is predominately expressed in HCC cells and its high expression is positively correlated with abnormal lipid metabolism and predicts the poor prognosis of HCC patients. Mechanical study indicates that ACSL3 could promote the synthesis of 1-palmitoyl-2-oleoyl-*sn*-glycero-3-phosphocholine (POPC), which could act as a signaling transduction molecule to activate peroxisome proliferator-activated receptor α (PPARα) pathway and enhance the transcription of downstream lipid metabolism-associated genes [30–33], thereby promoting HCC growth and metastasis via accelerating lipid catabolism and anabolism. As an important lipid metabolism-associated factor, the specific regulatory mechanism of ACSL3 in HCC development and progression remains unclear. Our work first systemically uncovers the biological function and molecular mechanism of ACSL3 in promoting HCC growth and metastasis. Considering the lack of specific inhibitor for ACSL3, we further construct an endosomal pH-responsive nanoplatform for systemic delivery of ACSL3 siRNA (siACSL3), and demonstrate its ability to efficiently silence ACSL3 expression in vivo and inhibit HCC tumor growth and metastasis in both orthotopic and patient-derived xenograft (PDX) tumor models.

Materials and methods

Patients and tissue samples

Tumor samples of HCC patients ($n = 124$) were collected from the Department of Hepatobiliary Surgery of Sun Yat-Sen Memorial Hospital. Tumor samples include surgically resected tumor tissues from 116 HCC patients and the matched adjacent tissues, primary tumor tissues and postoperative lung metastatic tumor tissues from 8 HCC patients. All samples were collected with the informed consent of the patients in accordance with the International Ethical Guidelines for Biomedical Research Involving Human Subjects (CIOMS). The study was approved by the Institutional Review Board (IRB) of Sun Yat-Sen Memorial Hospital.

High-throughput proteomics

The matched primary tumor tissues and postoperative lung metastatic tissues from three HCC patients were cut into tiny pieces and then immersed into 10 mL of Dulbecco's Modified Eagle Medium (DMEM) containing 5% fetal bovine serum (FBS), 2 mg/mL collagenase I, 0.4 mg/mL pronase, and 2 mg/mL hyaluronidase. After shaking at 37 °C for 2 h, the mixture was centrifuged (1000 rpm, 10 min) and the obtained cell cluster was washed with cold phosphate-buffered saline (PBS) solution thrice. Subsequently, the cell cluster was dispersed in lysis buffer and the supernatant was collected by centrifugation (12000 rpm, 10 min). The protein concentration in the obtained supernatant was determined by bicinchoninic acid (BCA) assay and equal amount of proteins was subjected for proteomics analysis using the Data independent acquisition (DIA) method, in which all ions within a selected m/z range are fragmented and analyzed in a second stage of tandem mass spectrometry. The final protein expression profile was analyzed by Proteome Discoverer Software (ver. 2.4) containing a complex proteomic standard.

scRNA-seq data analysis

The scRNA-seq results of the public GSE146115 dataset containing 3134 cells from four HCC patients were downloaded from the Tumor ImmunoSingle Cell Center 2.0 (TISCH 2.0) database (http://tisch.comp-genomics.org/) [34, 35], which has been completed with a st andard scRNA-seq workflow, including quality control, normalization, unsupervised clustering and cell type annotation. The cell classification and gene expression distribution maps were visualized using the functions such as hdf5r, Seurat, ggplot2, and readxl in R language version 4.4.2. Subsequently, the malignant cell population was extracted, in which the cells expressing ACSL3 higher than the mean ACSL3 expression level of total cells was defined as the high-expression group, while the cells expressing ACSL3 lower than the mean ACSL3 expression level was defined as the low-expression group. The differentially expressed genes (DEGs) between these two groups were identified using the FindMarkers function (logfc.threshold = 0.25, min.pct = 0.1), and then were applied for Gene Ontology (GO) analysis. To further examine ACSL3 expression in the subpopulation of malignant cells, the FindAllMarkers function was used to analyze the expression of the typical genes associated with each subpopulation (logfc.threshold = 1 and min.pct = 0.3). The top 2 genes in the avg_log2FC ranking were identified as the typical genes of each cell subpopulation. Subsequently, the FetchData function was employed to analyze ACSL3 expression level in each cell subpopulation.

Online dataset

The correlation of ACSL3 expression in the tumor tissues of HCC patients with their survival outcome was downloaded from TCGA database. Kaplan-Meier curve and log-rank test were used to compare overall survival (OS) and disease-specific survival (DSS) in different patient groups.

Cell culture

HCC cells (MHCC-97H, MHCC-97L, HepG2, Huh7, HCC-LM3) were incubated in DMEM supplemented with 10% FBS and cultured at 37 °C in a humidified atmosphere containing 5% CO_2. The cells were tested every one month to ensure no Mycoplasma contamination using Mycoplasma Detection Kit (Solarbio, China).

ACSL3 silencing and up-regulation

MHCC-97H and Huh7 cells were respectively seeded in 6-well plates at a density of 50,000 cells/well and incubated in 2 mL of DMEM containing 10% FBS for 24 h. Subsequently, Lipo3k/siACSL3 complexes or NPs(siACSL3) were added at a siRNA concentration of 30 nM. After 24 h incubation, the cells were washed with PBS solution and further incubated in fresh medium for another 48 h. Thereafter, the total RNA was extracted using Trizol for reverse transcription quantitative polymerase chain reaction (qRT-PCR) analysis. The total protein was also extracted using lysis buffer supplemented with protease inhibitor cocktail and phosphatase inhibitors for western blot analysis. To up-regulate ACSL3 expression, HepG2 cells were seeded in 6-well plates at a density of 50,000 cells/well and incubated in 2 mL of DMEM containing 10% FBS for 24 h. Subsequently, Lipo3k/ACSL3-expressing plasmid complexes were added at a plasmid concentration of 1 μg/mL. After 24 h incubation, the cells were washed with PBS solution and further incubated in fresh medium for another 48 h. The total RNA and proteins were extracted for qRT-PCR and western blot analysis.

Transcriptome sequencing

MHCC-97H cells were seeded in 6-well plates at a density of 50,000 cells/well and ACSL3 expression was silenced with the Lipo3k/siACSL3 complexes using the method aforementioned. The total RNA was extracted with Trizol and then subjected for RNA sequencing analysis (Beijing Genomics Institution, China). Gene enrichment analysis was performed using the company's online interaction analysis system.

Detection of intracellular metabolites

MHCC-97H and Huh7 cells were respectively seeded in 6-well plates at a density of 50,000 cells/well and ACSL3 expression was silenced with the Lipo3k/siACSL3

complexes using the method described above. Thereafter, the cells were trypsinized and collected by centrifugation (1000 rpm, 3 min). After washing with PBS and then deionized water containing 5% mannitol, the cells were dispersed into the mixture of water, methanol, and acetonitrile (volume ratio, 1/2/2). After repeated freezing in the liquid nitrogen and thawing at room temperature, the mixture was centrifuged at 4 °C (12000 rpm, 30 min) and the NADH/NAD^+, ATP/ADP and acetyl-CoA were detected using the commercially available kits. The amount of DAG, TAG, and POPC in the supernatant was also examined by liquid chromatography mass spectrometry (LC-MS, Shimadzu LC-20AB, Japan).

Detection of intracellular lipid droplets

MHCC-97H and Huh7 cells were respectively seeded in round discs at a density of 50,000 cells/well and ACSL3 expression was silenced with the Lipo3k/siACSL3 complexes using the method described above. Subsequently, the cells were stained with BODIPY 493/503 (#D3922, Invitrogen, USA) and intracellular lipid droplets were observed under a ZEISS 800 confocal laser scanning microscope (CLSM).

Animals

BALB/c nude mice and NSG (NOD/SCID/IL2Rγ^{null}) mice (4–5 weeks old) were purchased from the Sun Yat-Sen University Experimental Animal Center (Guangzhou, China). All in vivo studies were performed by a protocol approved by the Institutional Animal Care and Use Committee at Sun Yat-Sen Memorial Hospital.

Inhibition of orthotopic tumor growth and metastasis

MHCC-97H orthotopic tumor-bearing mice were randomly divided into four groups ($n = 5$) and given an intravenous injection of either (i) PBS; (ii) naked siACSL3; (iii) NPs(siCTL) or (iv) NPs(siACSL3) at a dose of 1 nmol siRNA per mouse once every two days. All the mice were administrated three consecutive injections and the tumor growth was monitored by bioluminescence imaging. The tumors and lungs were collected and sectioned for histological analysis.

Inhibition of PDX tumor growth

PDX tumor-bearing mice were randomly divided into four groups ($n = 5$) and given an intravenous injection of either (i) PBS; (ii) naked siACSL3; (iii) NPs(siCTL) or (iv) NPs(siACSL3) at a dose of 1 nmol siRNA per mouse once every two days. All the mice were administrated three consecutive injections and the tumor growth was monitored every 2 days by measuring perpendicular diameters with a caliper. Tumor volume was calculated as $V = W^2 \times L/2$, where W and L are the shortest and longest diameters, respectively. At the experimental endpoint, the tumors were collected and sectioned for histological analysis.

Statistical analysis

The in vitro data were presented as mean ± S.D. of three independent experiments. Statistical analysis was performed using SPSS 16.0 statistical software package and Graphpad Prism 8. Unpaired two-sided Student's t-test and one-way ANOVA were used to compare the cell and animal experiments with different treatments, and post hoc tests were employed to analyze difference between groups. In all cases, * $p < 0.05$, ** $p < 0.01$, and *** $p < 0.001$.

Results

High ACSL3 expression is positively correlated with metastasis and poor prognosis of HCC patients

To explore the key factors regulating HCC metastasis, we collected the matched primary tumor tissues and postoperative lung metastatic tumor tissues from three HCC patients (Table S1), and analyzed their proteomics profiles. As shown in Fig. 1A, ACSL3 is particularly noted among the top five differentially expressed proteins (i.e., ACSL3, ATAD5, COBL, TIM9, and SKT), as hazard ratio (HR) for the overall survival of cancer patients in The Cancer Genome Atlas (TCGA) database indicates that ACSL3 is the key risk factor for various cancer types especially HCC (Fig. 1B). We also analyzed the scRNA-seq results of four HCC patients from the public GSE146115 dataset [34], in which ACSL3 is predominately expressed in HCC cells (Fig. 1C and D, Fig. S1) and high ACSL3 expression indicates active lipid metabolism (Fig. 1E) and strong proliferation and metastasis ability of HCC cells (Fig. 1F). The similar tendency could be also found in TCGA database, in which high ACSL3 expression is positively correlated with the expression of proliferation marker (Ki-67, Fig. S2A) and proliferating cell nuclear antigen (PCNA, Fig. S2B) in HCC patients. Moreover, the results in TCGA database also show that ACSL3 is highly expressed in the tumor tissues of HCC patients compared to normal liver tissues (Fig. 1G) and the expression level of ACSL3 shows an upward trend as the malignancy of HCC increases (Fig. S3). More importantly, HCC patients with high ACSL3 expression in TCGA database have poor overall survival (OS, Fig. 1H) and disease specific survival (DSS, Fig. 1I). To further explore the clinical correlation between ACSL3 and HCC, we examined ACSL3 expression in the matched adjacent, primary, and lung metastatic tumor tissues of HCC patients ($n = 8$). As presented in Fig. 1J and K, ACSL3 is highly expressed in the tumor tissues and its expression level further increases in the metastatic tumor tissues. With this information, we further examined ACSL3 expression in tumor tissues of 116 HCC patients (Table S2) and analyzed the influence of ACSL3 expression on their prognosis. Similar as

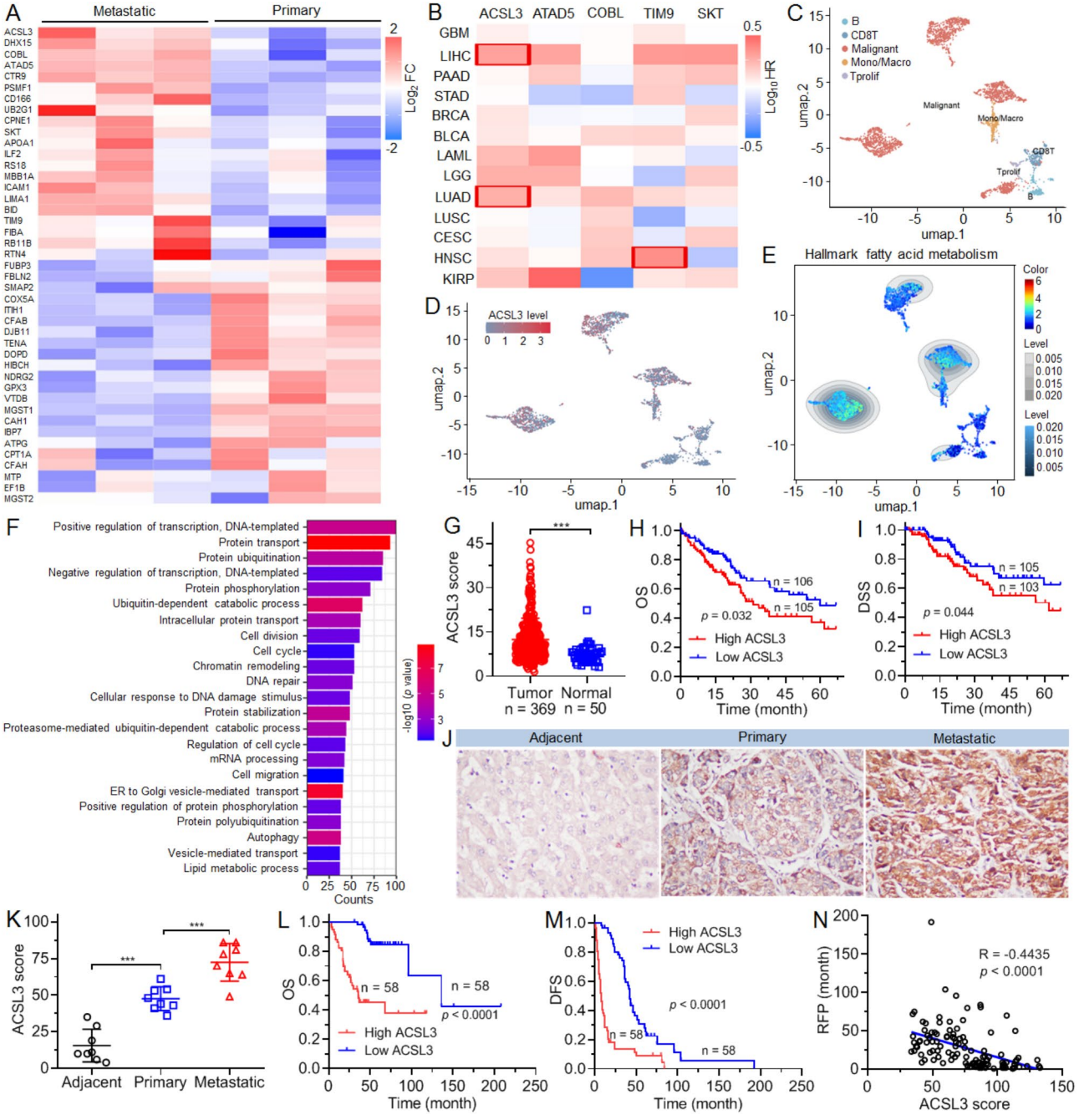

Fig. 1 ACSL3 is highly expressed in the metastatic tumor tissues of HCC patients and positively correlated with the activity of lipid metabolism and poor prognosis HCC patients. (**A**) Heatmap of differentially expressed proteins in the matched primary and postoperative lung metastatic tumor tissues of three HCC patients. (**B**) TCGA database showing the HR of top five genes (ACSL3, ATAD5, COBL, TIM9, and SKT) for the overall survival of cancer patients. (**C-E**) UMAP visualization (**C**), ACSL3 expression level (**D**), and lipid metabolism level (**E**) of total cell types in the tumor tissues of four HCC patients in GSE146115 dataset. (**F**) GO analysis of DEGs in the tumor cells of four HCC patients in GSE146115 dataset. (**G**) TCGA database showing ACSL3 expression in normal liver tissues ($n = 50$) and tumor tissues ($n = 369$) of HCC patients. (**H, I**) TCGA database showing OS (**H**) and DSS (**I**) of HCC patients with different ACSL3 expression levels. (**J**) Immunohistochemistry (IHC) analysis of ACSL3 expression in the matched adjacent, primary, and postoperative lung metastatic tumor tissues of one HCC patient. (**K**) ACSL3 score determined by IHC analysis of the matched adjacent, primary, and postoperative lung metastatic tumor tissues of HCC patients ($n = 8$). (**L, M**) OS (**L**) and DFS (**M**) of HCC patients ($n = 116$) with different ACSL3 expression levels. (N) RFP of HCC patients ($n = 116$) with different ACSL3 scores. *** $p < 0.001$

the tendency in TCGA database, HCC patients with high ACSL3 expression show a poor prognosis, as demonstrated by poor OS (Fig. 1L) and DFS (Fig. 1M). Moreover, high ACSL3 expression could be observed in the tumor tissues of HCC patients with short recurrence-free period (RFP) (Fig. 1N). All these results indicate that high ACSL3 expression is closely associated with the active lipid metabolism and positively correlated with the progression and poor prognosis of HCC patients.

High ACSL3 expression promotes proliferation, migration, and invasion of HCC cells

After validating the clinical significance of ACSL3 in HCC patients, we next investigated its function to regulate the biological behaviors of HCC cells. To this end, we chose MHCC-97H cells, a type of HCC cell line with high ACSL3 expression (Fig. S4), and then used siACSL3 to silence ACSL3 expression (Fig. 2A and B). As shown in Fig. 2C and D, ACSL3 silencing could not only inhibit the proliferation and clone formation of MHCC-97H

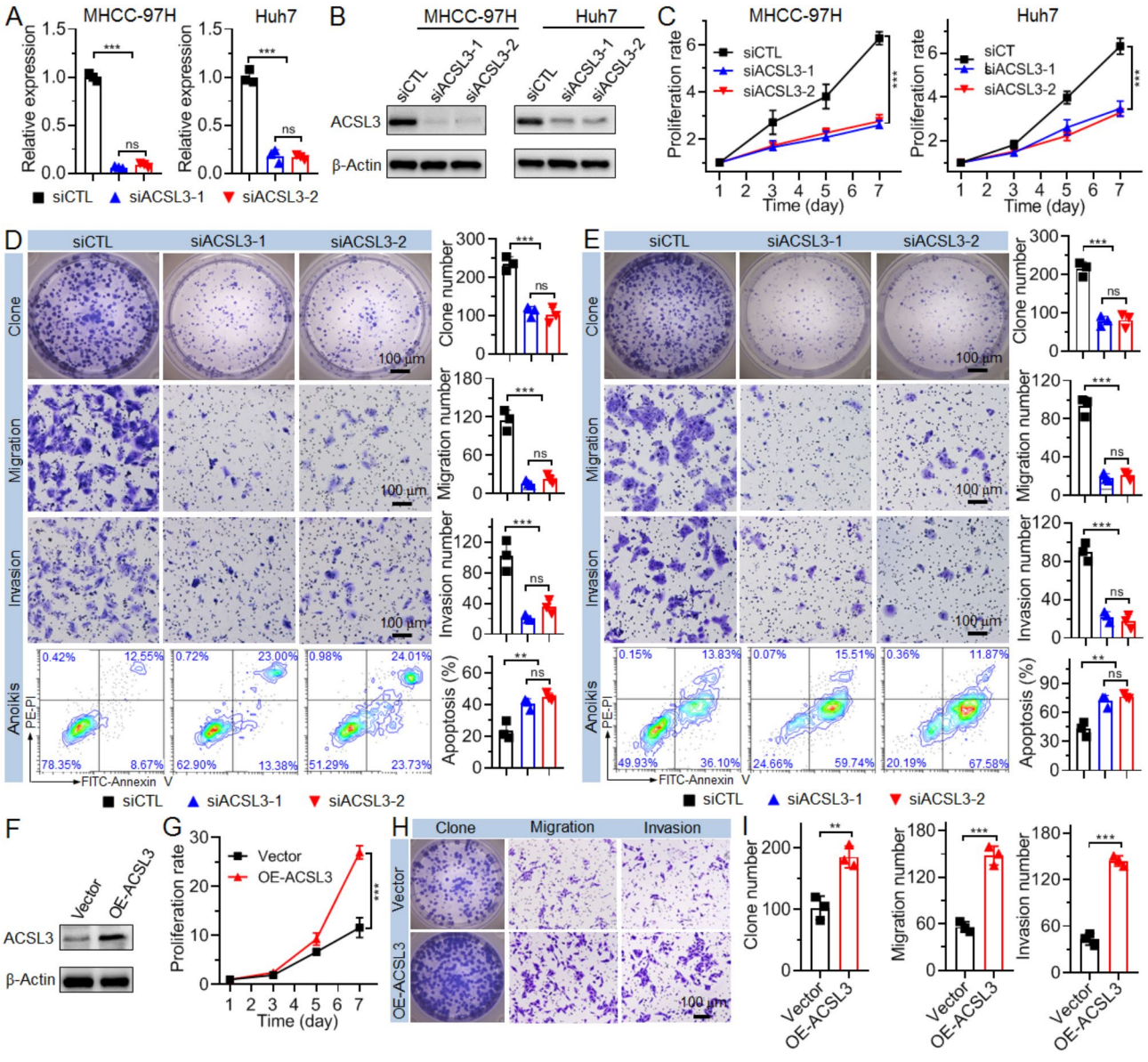

Fig. 2 High ACSL3 expression promotes the proliferation, migration, and invasion of HCC cells. (**A, B**) qRT-PCR (**A**) and western blot (**B**) analysis of ACSL3 expression in MHCC-97H and Huh7 cells treated with siACSL3 at a concentration of 30 nM. (**C**) Proliferation profiles of MHCC-97H and Huh7 cells treated with siACSL3 at a concentration of 30 nM. (**D, E**) Clone formation, migration, invasion, anoikis and the statistic results of MHCC-97H (**D**) and Huh7 cells (**E**) treated with siACSL3 at a concentration of 30 nM. (**F**) Western blot analysis of ACSL3 expression in HepG2 cells treated with the ACSL3-expressing plasmid (OE-ACSL3) at a plasmid concentration of 1 μg/mL. (**G-I**) Proliferation profile (**G**) and clone formation, migration, invasion (**H**) and the statistic results (**I**) of HepG2 cells treated with the ACSL3-expressing plasmid at a plasmid concentration of 1 μg/mL. *ns*, no significance; ** $p < 0.01$; *** $p < 0.001$

cells, but also significantly weaken their invasion, migration, and anoikis resistance ability. These results imply the important role of ACSL3 in regulating the growth and metastasis of HCC cells. To further demonstrate this statement, we silenced ACSL3 expression in another HCC cell line (i.e., Huh7 cells). Similarly, the proliferation, clone formation, invasion, migration, and anoikis resistance ability of Huh7 cells is significantly impaired after silencing ACSL3 expression (Fig. 2C and E). In addition, we also chose HepG2 cells with low ACSL3 expression (Fig. S4) and evaluated the influence of ACSL3 up-regulation on their biological behaviors (Fig. 2F). From the results displayed in Fig. 2G-I, ACSL3 up-regulation could dramatically promote the proliferation, clone formation, migration, and invasion of HepG2 cells. Besides examining the function of ACSL3 in vitro, we also intravenously injected the luciferase (Luc)-expressed MHCC-97H cells with lentivirus-mediated stable ACSL3 silencing by shRNA into healthy mice to investigate the influence of ACSL3 on the growth and metastasis of HCC cells in vivo. As shown in Fig. 3A-C, much weaker bioluminescence could be observed in the whole body and collected lung tissues of mice received the injection of MHCC-97H cells with ACSL3 silencing, indicating that ACSL3 could indeed promote the proliferation and metastasis of HCC cells to form metastatic nodes. This tendency could be

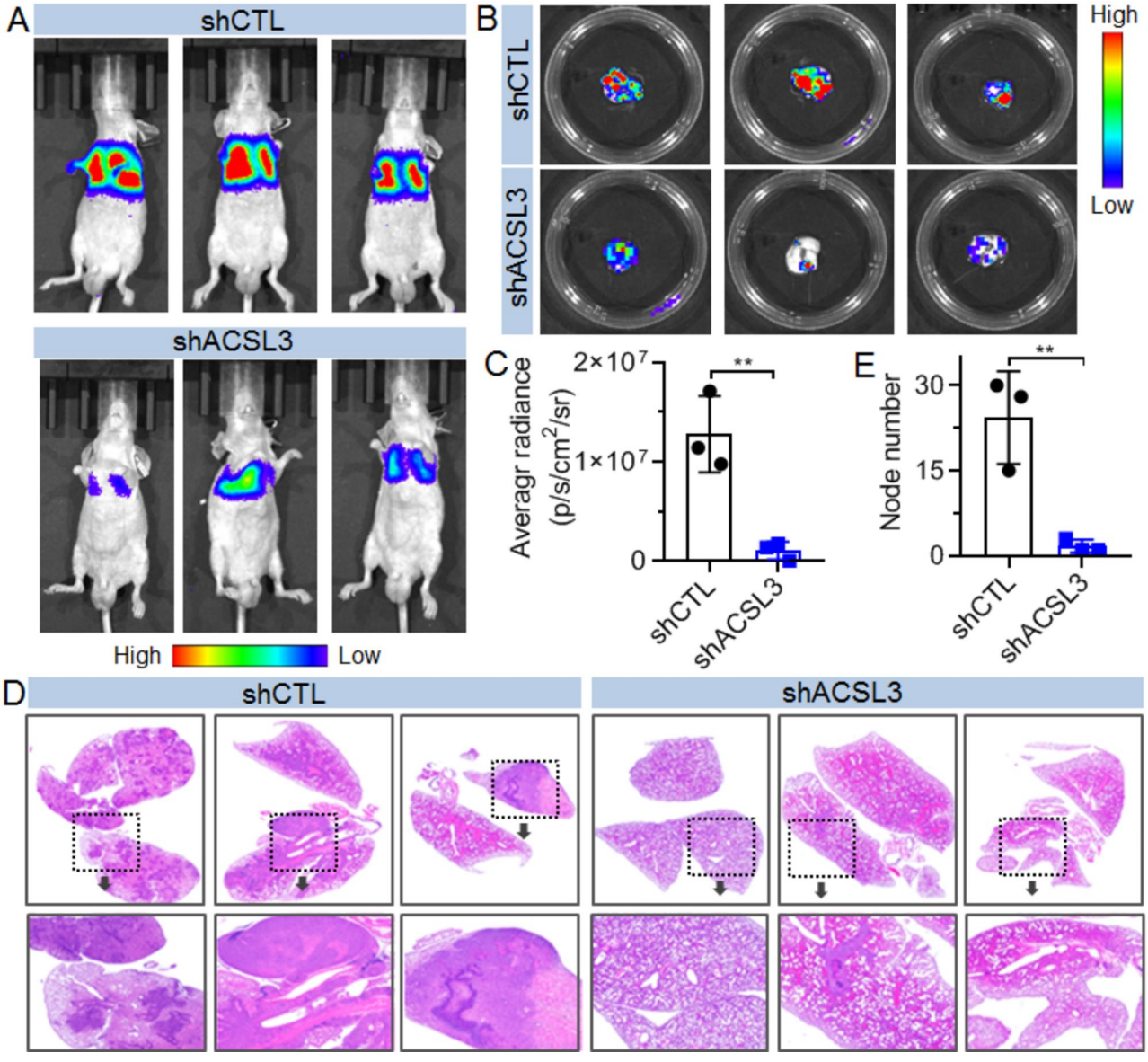

Fig. 3 High ACSL3 expression promotes HCC growth and metastasis. (**A-C**) Bioluminescence images of mice (**A**) and collected lung tissues (**B**) and the total radiance of tumor burden in the collected lung tissues (**C**) at day 42 post intravenous injection of Luc-MHCC-97H cells with ACSL3 silencing by shRNA. (**D, E**) Histological staining (**D**) and the statistic results of metastatic nodes in the collected lung tissues (**E**) shown in (**B**). ** $p < 0.01$

also found in the results of histological analysis (Fig. 3D and E), in which much less and smaller metastatic nodes are formed in the lung tissues of mice injected with MHCC-97H cells with ACSL3 silencing. All these results clearly indicate that high ACSL3 expression could promote HCC growth and metastasis.

High ACSL3 expression promotes POPC synthesis to activate PPARα and enhance lipid metabolism

Having confirmed the important role of ACSL3 in regulating HCC growth and metastasis, we next investigated the regulatory mechanism via examining the transcriptional information. The heatmap of DEGs in MHCC-97H cells before and after ACSL3 silencing is shown in Fig. 4A. Gene cluster analysis using the Kyoto Encyclopedia of

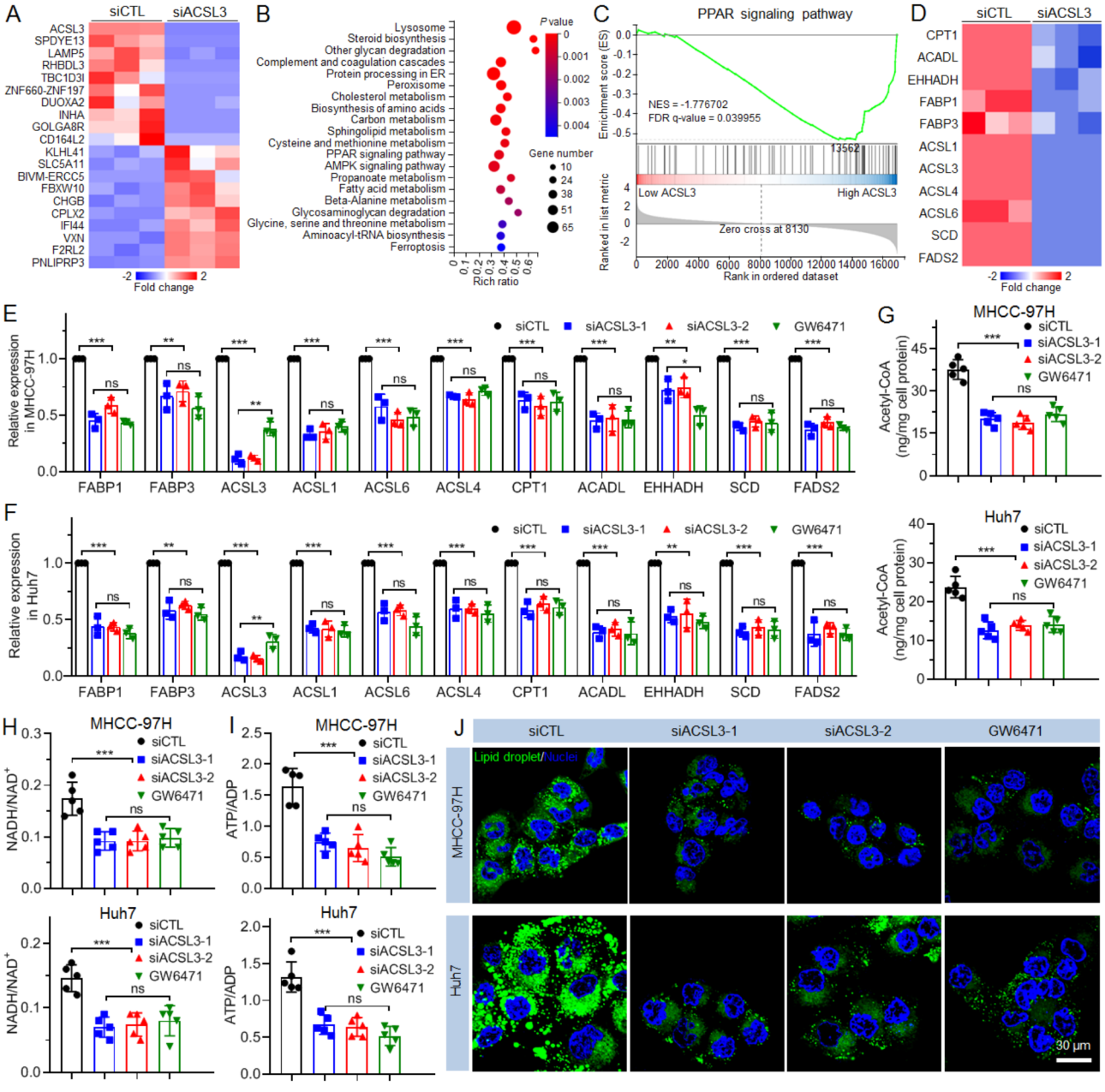

Fig. 4 High ACSL3 expression promotes lipid metabolism via enhancing the transcription of lipid metabolism-associated genes in HCC cells. (**A**) Heatmap of mRNA expression profile of MHCC-97H cells treated with siACSL3 at a concentration of 30 nM. (**B, C**) KEGG (**B**) and GSEA (**C**) analysis of the DEGs in MHCC-97 H cells treated with siACSL3 at a concentration of 30 nM. (**D**) Heatmap of the DEGs in the PPAR signaling pathway enriched in KEGG analysis shown in (**C**). (**E, F**) qRT-PCR analysis of expression of the DEGs shown in (**D**) in MHCC-97H (**E**) and Huh7 cells (**F**) treated with 30 nM siACSL3 or 20 μM PPARα inhibitor GW6471. (**G-J**) Production of acetyl-CoA (**G**), NADH (**H**) and ATP (**I**) and formation of lipid droplets (**J**) in MHCC-97H and Huh7 cells treated with 30 nM siACSL3 or 20 μM PPARα inhibitor GW6471. *ns*, no significance; ** $p < 0.01$; *** $p < 0.001$

Genes and Genomes (KEGG) reveals that these DEGs are mainly enriched in PPAR and metabolism-associated signaling pathways (Fig. 4B). In addition, GeneSet Enrichment Analysis (GSEA) analysis also indicates the negative regulation of PPAR pathway after ACSL3 silencing (Fig. 4C). With this information, we further analyzed the DEGs in the PPAR signaling pathway enriched in KEGG analysis. As presented in Fig. 4D, the DEGs are predominately associated with lipid metabolism including catabolism and anabolism [9], and their expression level is dramatically down-regulated after ACSL3 silencing (Fig. S5). This similar tendency could be also found in the results of qRT-PCR analysis (Fig. 4E and F). It is known that PPARs include three subtypes (i.e., PPARα, PPARδ, and PPARγ) and PPARα plays a crucial role in regulating cellular lipid metabolism via promoting the transcription of various genes (e.g., FABP1, FABP3, SCD, etc.) involved in lipid metabolism in the liver [31–33, 36]. Therefore, we speculate that high ACSL3 expression may activate PPARα pathway to promote the transcription of downstream lipid metabolism-associated genes, thereby leading to the enhanced lipid catabolism and anabolism. To validate this speculation, we employed the chromatin immunoprecipitation (ChIP) assay to examine the binding of PPARα to bind with DNA. The results clearly reveal the ability of PPARα to bind with the promoter regions of various lipid metabolism-associated genes in HCC cells (Fig. S6). In addition, we also used the inhibitor GW6471 to block PPARα activity in HCC cells and then examined the expression of lipid metabolism-associated genes. Similar as ACSL3 silencing, GW6471 treatment could also significantly down-regulate the expression of various lipid metabolism-associated genes in both MHCC-97H (Fig. 4E) and Huh7 cells (Fig. 4F). Due to the down-regulation of these genes, the level of lipid catabolism represented by acetyl coenzyme A (Acetyl-CoA, Fig. 4G), nicotinamide adenine dinucleotide (NADH, Fig. 4H), and ATP production (Fig. 4I) as well as lipid anabolism represented by lipid droplet formation (Fig. 4J) is dramatically suppressed in MHCC-97H and Huh7 cells treated with siACSL3 or GW6471.

After verifying the ability of ACSL3 to enhance lipid metabolism via activating PPARα pathway, we next explored how ACSL3 activates this pathway. We first examined PPARα expression in HCC cells before and after ACSL3 silencing. As shown in Fig. 5A and B, there is nearly no change in PPARα expression at both mRNA and protein level in MHCC-97H and Huh7 cells. It has been reported that PPARα is a nuclear hormone receptor and its activity could be regulated at multiple levels, including gene expression, protein translation, post-translational modifications, and ligand activation [32, 33]. Currently, the reported endogenous activating ligands of PPARα mainly includes fatty acids (e.g., arachidonic acid), eicosanoids (e.g., leukotrienes), phosphatidylcholines (e.g., POPC), and polyphenols (e.g., resveratrol) [33, 37]. As a classic enzyme, ACSL3 can catalyze free long-chain fatty acids into fatty acyl-CoA esters that can be converted into various lipids and their derivatives, such as lysophosphatidic acid (LPA), phosphatidic acid (PA), diacylglycerol (DAG), and triacylglyceride (TAG) [24, 38, 39]. More importantly, in the ACSL family, only ACSL3 shows the specific function in promoting the production of phosphatidylcholines including POPC [38–40]. Furthermore, as the precursor for the synthesis of all the endogenous phosphatidylcholines, recent studies have revealed that DAG can be converted into POPC to activate PPARα pathway [31–33]. Inspired by these pioneered results, we speculate that high ACSL3 expression may promote the synthesis of DAG and the subsequent POPC to activate PPARα and enhance the transcription of downstream genes. To verify our hypothesis, we used mass spectrometry to detect the amount of DAG and POPC in HCC cells. Indeed, silencing ACSL3 expression in MHCC-97H and Huh7 cells could induce around 2-fold decease in DAG production (Fig. 5C) and 2-fold decrease in POPC production (Fig. 5D). With this encouraging result, we examined the expression of lipid metabolism-associated genes in HCC cells treated with siACSL3 followed by addition of exogenous POPC. As shown in Fig. 5E and F, addition of exogenous POPC could rescue the expression of various lipid metabolism-associated genes, thus inducing increased ATP production (Fig. 5G) and lipid droplet formation (Fig. 5H) in both MHCC-97H and Huh7 cells. Based on these results, we conclude that high ACSL3 expression could promote POPC synthesis to activate PPARα pathway and enhance the transcription of various downstream lipid metabolism-associated genes, thereby leading to enhanced lipid catabolism and anabolism to promote HCC growth and metastasis (Fig. 5I).

NPs-mediated ACSL3 silencing inhibits proliferation, migration, and invasion of HCC cells

Based on the important role of ACSL3 in promoting HCC growth and metastasis, targeted inhibition of its expression could be a promising strategy for effective HCC therapy. Nucleic acid drugs such as siRNAs can be used to achieve this goal due to their unique characteristic of silencing any target genes [41, 42]. However, naked siRNAs belong to negatively charged biomacromolecules and specific delivery tools are required to enhance their cytosolic transport [43–45]. To this end, we constructed an endosomal pH-responsive NP platform for systemic siACSL3 delivery. The nanoplatform is made with a pH-responsive polymer Meo-PEG-*b*-PDPA with a pK_a (~6.34, Fig. S7-S10) close to endosomal pH [46–48] and an amphiphilic cationic compound G0-C14

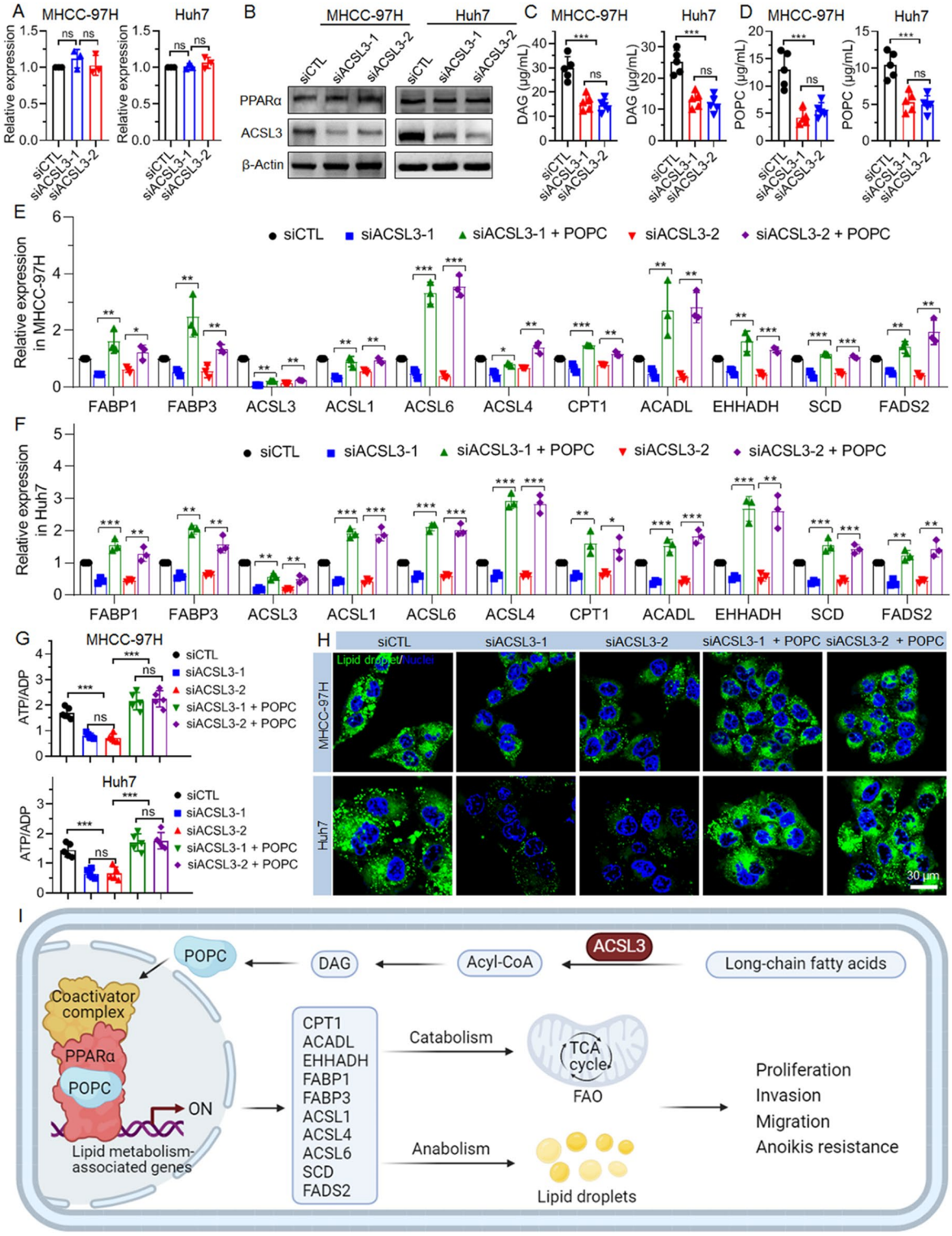

Fig. 5 High ACSL3 expression promotes POPC synthesis to activate PPARα and enhance the transcription of downstream lipid metabolism-associated genes. (**A, B**) qRT-PCR (**A**) and western blot (**B**) analysis of PPARα expression in MHCC-97H and Huh7 cells treated with siACSL3 at a concentration of 30 nM. (**C, D**) Intracellular concentration of DAG (**C**) and POPC (**D**) determined by MS analysis of MHCC-97H and Huh7 cells treated with siACSL3 at a concentration of 30 nM. (**E, F**) qRT-PCR analysis of the expression of lipid metabolism-associated genes in MHCC-97H (**E**) and Huh7 cells (**F**) treated with 30 nM siACSL3 followed by 50 μM POPC. (**G, H**) ATP production (**G**) and formation of lipid droplets (**H**) in MHCC-97H and Huh7 cells treated with 30 nM siACSL3 followed by 50 μM POPC. (**I**) Schematic illustration of the regulatory mechanism of ACSL3 in promoting HCC growth and metastasis. High ACSL3 expression could promote POPC synthesis to activate PPARα and enhance the transcription of various downstream lipid metabolism-associated genes, which thereby accelerate lipid catabolism and anabolism to promote HCC growth and metastasis. *ns*, no significance; * $p < 0.05$; ** $p < 0.01$; *** $p < 0.001$

we previously developed (Fig. S11) [49, 50]. As shown in Fig. 6A, the polymer Meo-PEG-*b*-PDPA can self-assemble into stable NPs with hydrophilic PEG shells and hydrophobic PDPA cores, in which the charge-mediated complexes of siACSL3 and G0-C14 are entrapped [49–51]. By adjusting the N/P molar ratio between G0-C14 and siACSL3, well-defined siACSL3-loaded NPs (denoted NPs(siACSL3)) with an average size of ~70 nm could be formed at an N/P ratio of 20 (Fig. 6B and C). These NPs are stable at a physiological pH (Fig. S12), but could rapidly release the loaded siACSL3 at a pH of 6.0 (Fig. 6D) due to the protonation of PDPA polymer and subsequent NP dissociation [46]. More importantly, the protonation of PDPA polymer could induce the "proton sponge" effect to enhance the endosomal escape of loaded siACSL3 (Fig. S13) [52], which thereby significantly improve the gene silencing efficacy of NPs(siACSL3). As shown in Fig. 6E and F, ACSL3 expression in MHCC-97 H cells treated with the NPs(siACSL3) could be down-regulated by ~80% at a siACSL3 concentration of 30 nM. With this efficient ACSL3 silencing, the proliferation rate of MHCC-97H cells is dramatically suppressed (Fig. 6G). Similarly, MHCC-97 H cells treated with the NPs(siACSL3) show an impaired ability of clone formation, migration, invasion, and anoikis resistance (Fig. 6H) compared to the cells treated with the NPs loading scrambled siRNA (denoted NPs(siCTL)).

NPs-mediated ACSL3 silencing inhibits HCC tumor growth and metastasis

Having validated the ability of NPs(siACSL3) to silence ACSL3 expression in vitro, we next evaluated whether these NPs could effectively silence ACSL3 expression in vivo and inhibit HCC growth and metastasis. The pharmacokinetics was first investigated via intravenous injection of NPs(siACSL3) into healthy mice. As shown in Fig. 7A, because of surface PEG shells to impair blood clearance [53], the NPs could significantly prolong the blood circulation period of loaded siACSL3 and around 6% of loaded siACSL3 could be detected in the blood at 12 h post the injection. Due to this prolonged blood circulation, the loaded siACSL3 shows more than 5-fold higher accumulation in the tumor tissues of MHCC-97H xenograft tumor-bearing mice compared to naked siACSL3 (Fig. 7B and C), thereby leading to around 80% decrease in ACSL3 expression in the tumor tissues (Fig. S14). With these encouraging results, we finally established a HCC orthotopic tumor-bearing mouse model using Luc-expressing MHCC-97 H cells and examined the ability of NPs(siACSL3) to inhibit HCC growth and metastasis. As shown in Fig. 7D, the less tumor burden clearly indicates the ability of NPs(siACSL3) to effectively inhibit the tumor growth (Fig. S15). More importantly, compared to the mice treated with the NPs(siCTL), the NPs(siACSL3) could dramatically improve the survival of tumor-bearing mice (Fig. 7E) and suppress the metastasis of HCC tumor (Fig. 7F and G). The stronger anti-tumor ability of NPs(siACSL3) than other therapeutic formulas could be also found in the results of histological analysis (Fig. 7H), in which lower ACSL3 expression, more apoptosis (TUNEL), and less proliferation (Ki67) could be observed in the tumor tissues of mice treated with the NPs(siACSL3).

To further assess the therapeutic effect of NPs(siACSL3), we also established a PDX tumor-bearing mouse model using the surgically resected tumor tissues of HCC patients and then intravenously injected the NPs into mice (Fig. 8A). As presented in Fig. 8B and D, the NPs(siACSL3) could also significantly inhibit the growth of PDX tumors and there is around 3-fold increase in the tumor size within an evaluation period of 28 days. By contrast, the tumor size of mice treated with the NPs(siCTL) increases by around8-fold within the same evalution period (Fig. S16). In addtion, the results of histological analysis of tumor tissues (Fig. 8E) also demonstrate the stronger ability of NPs(siACSL3) to inhibit tumor growth than other therapeutic formulas. Notably, the administration of NPs(siACSL3) does not induce the decrease in the mouse body weight in both orthotopic and PDX tumor models (Fig. S17) and apparent histological change in the main organs (Fig. S18). These results imply the low in vivo toxicity of NPs(siACSL3), which is further proven by the normal liver and kidney parameters in the results of routine blood analysis (Fig. S19).

Discussion

Metastasis is the main cause of cancer mortality and accounts for 90% of cancer-associated deaths. Cancer metastasis is a complex process including multiple sequential and interrelated steps, in which epithelial-mesenchymal transition (EMT), tumor stemness, epigenetic modifications, and immune evasion are widely involved [54–56]. In recent years, increasing evidences have revealed that abnormal lipid metabolism plays a crucial role in the development and progression of HCC as the liver is the central organ for lipid storage and metabolism [14, 15]. Therefore, identifying the key factors regulating abnormal lipid metabolism and uncovering their regulatory mechanisms could facilitate the development of new therapeutic targets for effective HCC therapy. In this work, we examined the proteomics difference between the paired primary and metastatic tumor tissues of HCC patients and revealed the abnormally high expression of ACSL3 in the metastatic tumor tissues. Further analyzing the scRNA-seq results of HCC patients indicates that ACSL3 is predominately expressed in HCC cells and its high expression predicts more active lipid metabolism and poor prognosis of HCC patients.

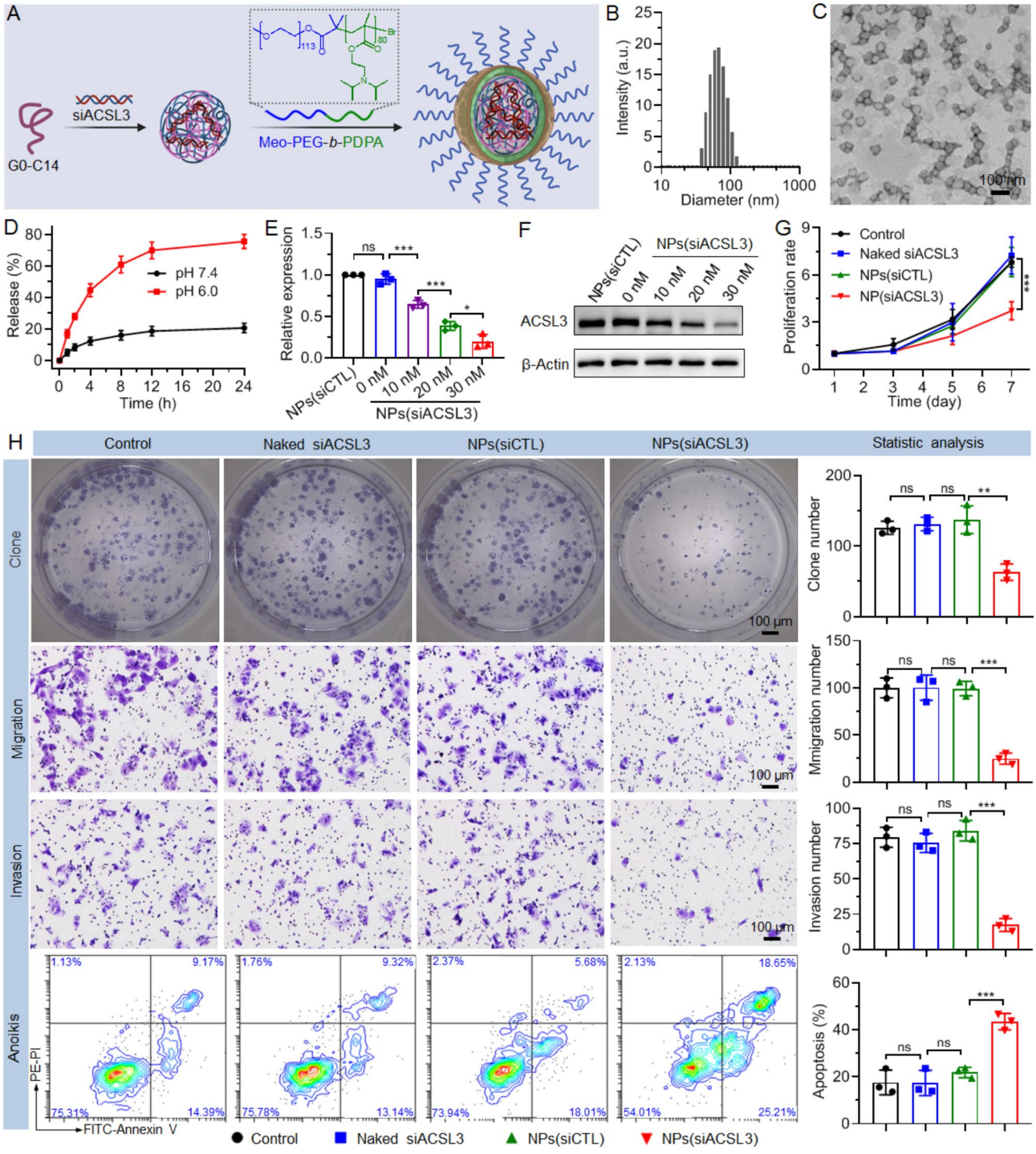

Fig. 6 NPs-mediated ACSL3 silencing inhibits the proliferation, migration, and invasion of HCC cells. (**A**) Schematic illustration of the endosomal pH-responsive nanoplatform made with the polymer Meo-PEG-*b*-PDPA and cationic lipid-like compound G0-C14. (**B, C**) Size distribution (**B**) and morphology (**C**) of the NPs(siACSL3) in aqueous solution. (**D**) Cumulative siACSL3 release from the NPs(siACSL3) in aqueous solution at pH 7.4 or 6.0. (**E, F**) qRT-PCR (**E**) and western blot (**F**) analysis of ACSL3 expression in MHCC-97H cells treated with the NPs(siACSL3) at different siACSL3 concentrations. (**G**) Proliferation of MHCC-97H cells treated with naked siACSL3, NPs(siCTL), or NPs(siACSL3) at a siRNA concentration of 30 nM. The cells incubated in blank culture medium were used as Control. (**H**) Clone formation, migration, invasion, anoikis, and the statistic results of MHCC-97H cells treated with the formulas shown in (**G**). *ns*, no significance; * $p < 0.05$; *** $p < 0.001$

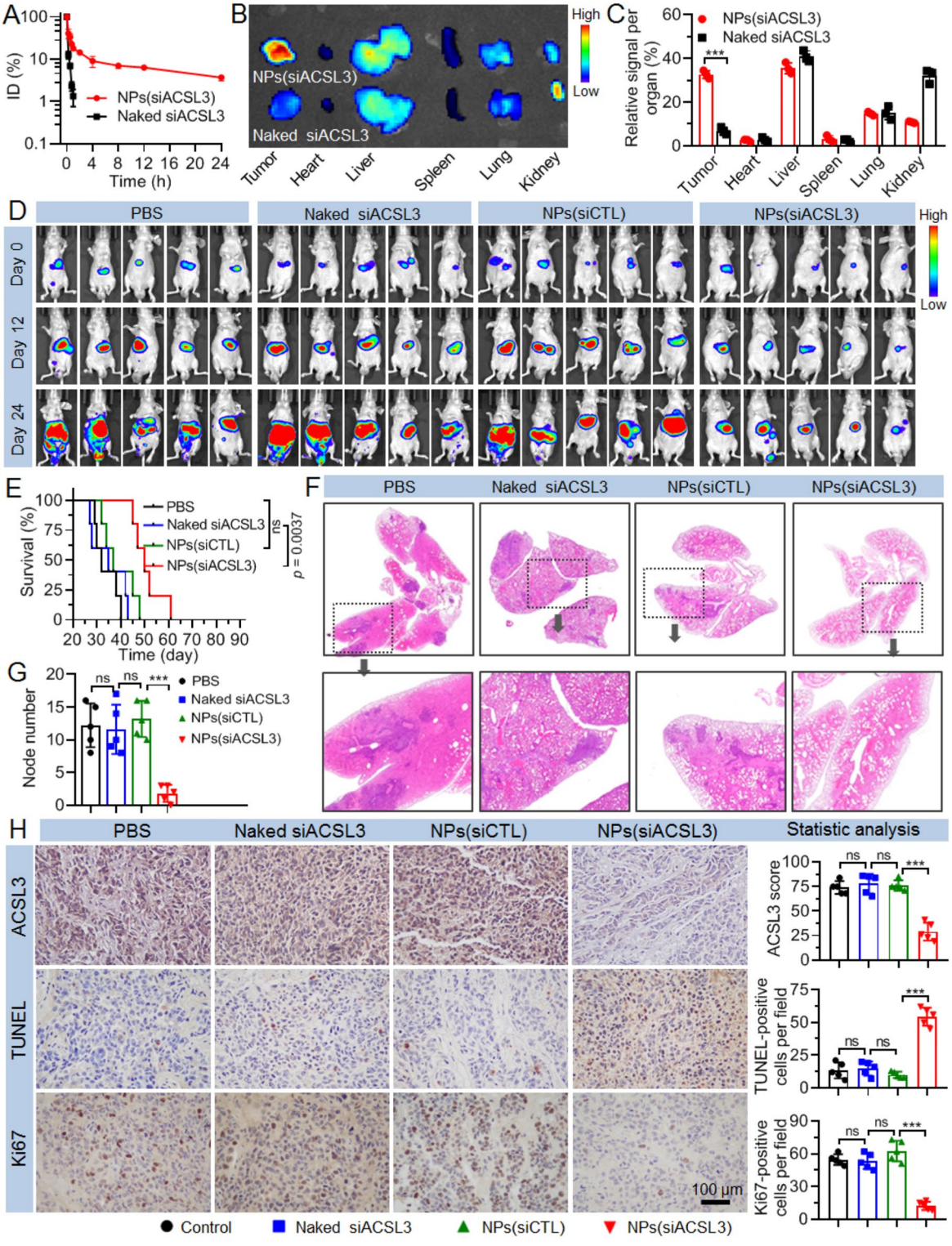

Fig. 7 NPs-mediated ACSL3 silencing inhibits HCC growth and metastasis in MHCC-97H orthotopic tumor model. (**A**) Blood circulation profile of naked siACSL3 and NPs(siACSL3). (**B, C**) Overlaid fluorescence image of the tumors and main organs (**B**) and biodistribution of naked siACSL3 and NPs(siACSL3) in MHCC-97H xenograft tumor-bearing mice sacrificed at 24 h post injection (**C**). (**D, E**) Bioluminescence images (**D**) and survival rate (**E**) of MHCC-97H orthotopic tumor-bearing mice treated with PBS, naked siACSL3, NPs(siCTL), or NPs(siACSL3). (**F, G**) Histological staining (**F**) and statistic results of metastatic nodes in the lung tissues (**G**) of MHCC-97H orthotopic tumor-bearing mice after systemic treatment in each group. (**H**) Expression of ACSL3, TUNEL, Ki67 and the statistical results determined by IHC staining analysis of the tumor tissues of mice after systemic treatment in each group. *ns*, no significance; *** $p < 0.001$

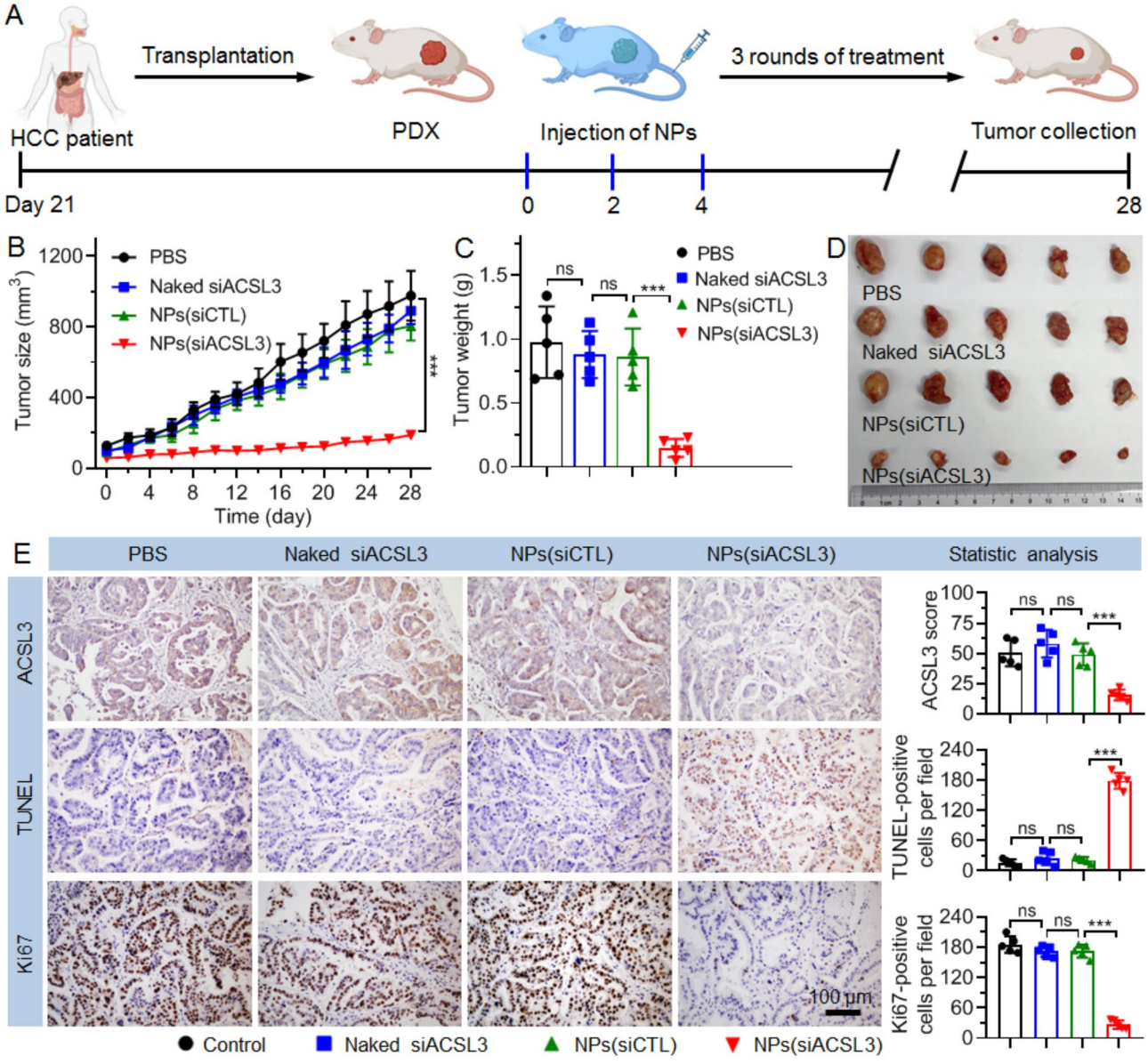

Fig. 8 NPs-mediated ACSL3 silencing inhibits HCC growth in PDX tumor model. (**A**) Schematic illustration of PDX tumor inoculation and treatment of PDX tumor-bearing mice. 21 days after tumor inoculation, tumor-bearing mice were treated with PBS, naked siACSL3, NPs(siCTL), or NPs(siACSL3). (**B-D**) Tumor growth (**B**), tumor weight (**C**), and the image of collected tumors (**D**) of PDX tumor-bearing mice treated with the formulas shown in (**A**). (**E**) Expression of ACSL3, TUNEL, Ki67 and the statistical results determined by IHC staining analysis of the tumor tissues of mice after systemic treatment in each group. *ns*, no significance; *** $p < 0.001$

As an important lipid metabolism-associated gene, ACSL3 can catalyze free long-chain fatty acids into fatty acyl-CoA esters, which can be converted into various lipids and their derivatives (e.g., PA, LPA, DAG, and TAG) for nutrient supply, signal transduction, and formation of cell structures [24]. Several recent studies have revealed that high ACSL3 expression could induce therapeutic resistance and promote the metastasis of skin, breast, pancreatic, and colorectal cancer via different regulatory mechanisms [57–59]. However, the function of ACSL3 in HCC remains elusive and the specific regulatory mechanism is also unclear. Our work indicates that high ACSL3 expression could promote the synthesis of POPC to activate PPARα, an important ligand-activated transcription factor that can regulate the transcription of various lipid metabolism-associated genes. To the best of our knowledge, our work first systemically elucidates the crucial function of ACSL3 to promote HCC growth and metastasis. As an important lipid metabolism-associated enzyme, ACSL3 may also promote HCC progression via other regulatory mechanisms as it has been demonstrated to regulate cancer progression via multiple

molecular mechanisms, such as the activiation of PPARγ in breast cancer and activiation of PPARδ in colorectal cancer. However, the results of our work indicate that the activation of PPARα pathway is the main reason for ACSL3 to promote HCC growth and metastasis.

At present, small molecule inhibitors are commonly used to inhibit the activity of target genes. As a polyunsaturated acid (PUFA) analogue, triacsin C is a widely used inhibitor for acyl-CoA synthetases including ACSL3 [60], which however may induce potential risks when using for systemic cancer treatment as triacsin C is a small chemical compound with low specificity and potential toxicity. RNA interference (RNAi) technology has been demonstrated as a powerful strategy for disease treatment due to its unique characteristic of silencing the expression of any target genes [41, 42]. More importantly, the use of NPs for in vivo delivery of RNAi agents such as siRNA significantly promotes the clinical translation of RNAi technology and several RNAi nanotherapeutics (e.g., Onpattro) have been already marketed [61, 62]. In addition, some other anticancer RNAi nanotherapeutics (e.g., TKM-080301 and STP707) are under clinical trials [63]. We had previously developed various stimuli-responsive NPs for systemic siRNA delivery and cancer therapy. These NPs can employ their stimuli-responsive characteristics to promote intracellular siRNA delivery and thus enhance anticancer effect [46–51]. Among them, endosomal pH-responsive NPs are particularly beneficial for systemic delivery of biomacromolecules (e.g., siRNA, mRNA, and proteins) that function in the cytoplasm. Therefore, we used this endosomal pH-responsive nanoplatform for systemic siACSL3 delivery and evaluated their ability to inhibit HCC growth and metastasis. Moreover, in order to impair the potential side effects of this siRNA delivery system, we used the BLAST test to choose the sequences matched with the transcript of ACSL3 gene and we designed three siACSL3 sequences, in which the siACSL3 sequence with the highest gene silencing efficacy was encapsulated into the NPs. Our results demonstrate that this siRNA delivery system does not induce apparent in vivo toxicity and could significantly inhibit HCC growth and metastasis. Notably, from the standpoint of clinical translation, although the NPs-mediated siACSL3 delivery shows a great potential for HCC therapy, especially the inhibition of HCC growth and metastasis, much more efforts are still needed to systemically evaluate the chronic in vivo toxicity.

Conclusions

We have revealed the important role of ACSL3 in promoting HCC growth and metastasis. Mechanically, ACSL3 could promote POPC synthesis to activate PPARα and enhance the transcription of various downstream lipid metabolism-associated genes, thereby promoting the growth and metastasis of HCC via accelerating lipid catabolism and anabolism. Systemic siACSL3 delivery with the endosomal pH-responsive NPs could effectively silence ACSL3 expression in vivo, leading to a significant inhibition of HCC growth and metastasis in orthotopic and PDX tumor models. Collectively, ACSL3 could be used a biomarker to predict the prognosis of HCC patients and the strategy of NPs-mediated ACSL3 silencing could be employed as a useful tool for HCC therapy.

Supplementary Information

The online version contains supplementary material available at https://doi.org/10.1186/s12943-025-02274-1 .

Supplementary Material 1

Author contributions

L.H., R.X., L.Z., and X.X. conceived the ideas and designed the experiments. L.H., R.X., S.C., C.L., W.L., S.L., and P.E.S performed the experiments. L.H., S.L., and L.Z. collected clinical samples. L.H., R.X., W.L., L.Z., and X.X. analyzed the data and wrote the manuscript. L.H., R.X., and S.C. contributed equally to this work.

Funding

The work was supported by the National Natural Science Foundation of China (82173392 and 82403670), the Guangdong Basic and Applied Basic Research Foundation (2024B1515040006 and 2022A1515110065), the Guangdong S&T Program (2023B1111030006), the grant from Guangzhou Science and Technology Bureau (2024A03J0846 and 20210303004), the Natural Science Foundation of Hunan Province (2023JJ50149), and the "Three million for Three Years" Project of the High-level Talent Special Funding Scheme of Sun Yat-Sen Memorial Hospital.

Data availability

No datasets were generated or analysed during the current study.

Declarations

Ethics approval and consent to participate

All HCC tumor samples were collected with the informed consent of the patients in accordance with the International Ethical Guidelines for Biomedical Research Involving Human Subjects (CIOMS). The study was approved by the Institutional Review Board (IRB) of Sun Yat-Sen Memorial Hospital. All animal experiments were performed by a protocol approved by the Institutional Animal Care and Use Committee at Sun Yat-Sen Memorial Hospital.

Competing interests

The authors declare no competing interests.

Received: 11 September 2024 / Accepted: 19 February 2025
Published online: 10 March 2025

References

1. Siegel RL, Miller KD, Wagle NS, Jemal A. Cancer statistics, 2023. CA Cancer Clin J. 2023;73:17–48.
2. Rumgay H, Arnold M, Ferlay J, Lesi O, Cabasag CJ, Vignat J, Laversanne M, McGlynn KA, Soerjomataram I. Global burden of primary liver cancer in 2020 and predictions to 2040. J Hepatol. 2022;77:1598–606.
3. Uka K, Aikata H, Takaki S, Shirakawa H, Jeong SC, Yamashina K, Hiramatsu A, Kodama H, Takahashi S, Chayama K. Clinical features and prognosis of patients with extrahepatic metastases from hepatocellular carcinoma. World J Gastroenterol. 2007;13:414–20.
4. Aino H, Sumie S, Niizeki T, Kuromatsu R, Tajiri N, Nakano M, Satani M, Yamada S, Okamura S, Shimose S, et al. Clinical characteristics and prognostic factors

for advanced hepatocellular carcinoma with extrahepatic metastasis. Mol Clin Oncol. 2014;2:393–8.
5. Jung SM, Jang JW, You CR, Yoo SH, Kwon JH, Bae SH, Choi JY, Yoon SK, Chung KW, Kay CS, Jung HS. Role of intrahepatic tumor control in the prognosis of patients with hepatocellular carcinoma and extrahepatic metastases. J Gastroenterol Hepatol. 2012;27:684–9.
6. Zanotelli MR, Zhang J, Reinhart-King CA. Mechanoresponsive metabolism in cancer cell migration and metastasis. Cell Metab. 2021;33:1307–21.
7. Hoy AJ, Nagarajan SR, Butler LM. Tumour fatty acid metabolism in the context of therapy resistance and obesity. Nat Rev Cancer. 2021;21:753–66.
8. Snaebjornsson MT, Janaki-Raman S, Schulze A. Greasing the wheels of the cancer machine: the role of lipid metabolism in cancer. Cell Metab. 2020;31:62–76.
9. Bian X, Liu R, Meng Y, Xing D, Xu D, Lu Z. Lipid metabolism and cancer. J Exp Med. 2020;218:e20201606.
10. Bergers G, Fendt SM. The metabolism of cancer cells during metastasis. Nat Rev Cancer. 2021;21:162–80.
11. DeBerardinis RJ, Chandel NS. Fundamentals of cancer metabolism. Sci Adv. 2016;2:e1600200.
12. Martínez-Reyes I, Chandel NS. Cancer metabolism: looking forward. Nat Rev Cancer. 2021;21:669–80.
13. Pavlova NN, Zhu J, Thompson CB. The hallmarks of cancer metabolism: still emerging. Cell Metab. 2022;34:355–77.
14. Bechmann LP, Hannivoort RA, Gerken G, Hotamisligil GS, Trauner M, Canbay A. The interaction of hepatic lipid and glucose metabolism in liver diseases. J Hepatol. 2012;56:952–64.
15. Satriano L, Lewinska M, Rodrigues PM, Banales JM, Andersen JB. Metabolic rearrangements in primary liver cancers: cause and consequences. Nat Rev Gastroenterol Hepatol. 2019;16:748–66.
16. Paul B, Lewinska M, Andersen JB. Lipid alterations in chronic liver disease and liver cancer. JHEP Rep. 2022;4:100479.
17. Wymann MP, Schneiter R. Lipid signalling in disease. Nat Rev Mol Cell Biol. 2008;9:162–76.
18. van Meer G, Voelker DR, Feigenson GW. Membrane lipids: where they are and how they behave. Nat Rev Mol Cell Biol. 2008;9:112–24.
19. Vogel FCE, Chaves-Filho AB, Schulze A. Lipids as mediators of cancer progression and metastasis. Nat Cancer. 2024;5:16–29.
20. Ma APY, Yeung CLS, Tey SK, Mao X, Wong SWK, Ng TH, Ko FCF, Kwong EML, Tang AHN, Ng IO, et al. Suppression of ACADM-mediated fatty acid oxidation promotes hepatocellular carcinoma via aberrant CAV1/SREBP1 signaling. Cancer Res. 2021;81:3679–92.
21. Hendrix S, Kingma J, Ottenhoff R, Valiloo M, Svecla M, Zijlstra LF, Sachdev V, Kovac K, Levels JHM, Jongejan A, et al. Hepatic SREBP signaling requires SPRING to govern systemic lipid metabolism in mice and humans. Nat Commun. 2023;14:5181.
22. Ito H, Nakamae I, Kato J-y, Yoneda-Kato N. Stabilization of fatty acid synthesis enzyme acetyl-CoA carboxylase 1 suppresses acute myeloid leukemia development. J Clin Invest. 2021;131:e141529.
23. Lally JSV, Ghoshal S, DePeralta DK, Moaven O, Wei L, Masia R, Erstad DJ, Fujiwara N, Leong V, Houde VP, et al. Inhibition of acetyl-CoA carboxylase by phosphorylation or the inhibitor ND-654 suppresses lipogenesis and hepatocellular carcinoma. Cell Metab. 2019;29:174–82.
24. Guertin DA, Wellen KE. Acetyl-CoA metabolism in cancer. Nat Rev Cancer. 2023;23:156–72.
25. Llovet JM, Kelley RK, Villanueva A, Singal AG, Pikarsky E, Roayaie S, Lencioni R, Koike K, Zucman-Rossi J, Finn RS. Hepatocellular carcinoma. Nat Rev Dis Primers. 2021;7:6.
26. Llovet JM, Bruix J. Molecular targeted therapies in hepatocellular carcinoma. Hepatology. 2008;48:1312–27.
27. Koboldt DC, Steinberg KM, Larson DE, Wilson RK, Mardis ER. The next-generation sequencing revolution and its impact on genomics. Cell. 2013;155:27–38.
28. Meyerson M, Gabriel S, Getz G. Advances in Understanding cancer genomes through second-generation sequencing. Nat Rev Genet. 2010;11:685–96.
29. Reuter Jason A, Spacek DV, Snyder Michael P. High-throughput sequencing technologies. Mol Cell. 2015;58:586–97.
30. Pascual G, Avgustinova A, Mejetta S, Martin M, Castellanos A, Attolini CS, Berenguer A, Prats N, Toll A, Hueto JA, et al. Targeting metastasis-initiating cells through the fatty acid receptor CD36. Nature. 2017;541:41–5.
31. Chakravarthy MV, Lodhi IJ, Yin L, Malapaka RRV, Xu HE, Turk J, Semenkovich CF. Identification of a physiologically relevant endogenous ligand for PPARα in liver. Cell. 2009;138:476–88.
32. Wang Y-X. PPARs: diverse regulators in energy metabolism and metabolic diseases. Cell Res. 2010;20:124–37.
33. Peters JM, Shah YM, Gonzalez FJ. The role of peroxisome proliferator-activated receptors in carcinogenesis and chemoprevention. Nat Rev Cancer. 2012;12:181–95.
34. Su X, Zhao L, Shi Y, Zhang R, Long Q, Bai S, Luo Q, Lin Y, Zou X, Ghazanfar S, et al. Clonal evolution in liver cancer at single-cell and single-variant resolution. J Hematol Oncol. 2021;14:22.
35. Han Y, Wang Y, Dong X, Sun D, Liu Z, Yue J, Wang H, Li T, Wang C. TISCH2: expanded datasets and new tools for single-cell transcriptome analyses of the tumor microenvironment. Nucleic Acids Res. 2022;51:D1425–31.
36. Rakhshandehroo M, Knoch B, Müller M, Kersten S. Peroxisome proliferator-activated receptor alpha target genes. PPAR Res. 2010, 2010:612089.
37. Bougarne N, Weyers B, Desmet SJ, Deckers J, Ray DW, Staels B, De Bosscher K. Molecular actions of PPARα in lipid metabolism and inflammation. Endocr Rev. 2018;39:760–802.
38. Currie E, Schulze A, Zechner R, Walther Tobias C. Farese Robert V: cellular fatty acid metabolism and cancer. Cell Metab. 2013;18:153–61.
39. Quan J, Cheng C, Tan Y, Jiang N, Liao C, Liao W, Cao Y, Luo X. Acyl-CoA synthetase long-chain 3-mediated fatty acid oxidation is required for TGFbeta1-induced epithelial-mesenchymal transition and metastasis of colorectal carcinoma. Int J Biol Sci. 2022;18:2484–96.
40. Fujimoto Y, Itabe H, Kinoshita T, Homma KJ, Onoduka J, Mori M, Yamaguchi S, Makita M, Higashi Y, Yamashita A, Takano T. Involvement of ACSL in local synthesis of neutral lipids in cytoplasmic lipid droplets in human hepatocyte HuH7. J Lipid Res. 2007;48:1280–92.
41. Setten RL, Rossi JJ, Han S-p. The current state and future directions of RNAi-based therapeutics. Nat Rev Drug Discov. 2019;18:421–46.
42. Hannon GJ. RNA interference. Nature. 2002;418:244–51.
43. Whitehead KA, Langer R, Anderson DG. Knocking down barriers: advances in siRNA delivery. Nat Rev Drug Discov. 2009;8:129–38.
44. Dong Y, Siegwart DJ, Anderson DG. Strategies, design, and chemistry in siRNA delivery systems. Adv Drug Deliv Rev. 2019;144:133–47.
45. Zhou Z, Liu X, Zhu D, Wang Y, Zhang Z, Zhou X, Qiu N, Chen X, Shen Y. Nonviral cancer gene therapy: delivery cascade and vector nanoproperty integration. Adv Drug Deliv Rev. 2017;115:115–54.
46. Xu R, Huang L, Liu J, Zhang Y, Xu Y, Li R, Su S, Xu X. Remodeling of mitochondrial metabolism by a mitochondria-targeted RNAi nanoplatform for effective cancer therapy. Small. 2024;20:2305923.
47. Yang K, Xu L, Xu Y, Shen Q, Qin T, Yu Y, Nie Y, Yao H, Xu X. Nanoparticles (NPs)-mediated LncBCMA Silencing to promote eEF1A1 ubiquitination and suppress breast cancer growth and metastasis. Acta Pharma Sin B. 2023;13:3489–502.
48. Huang Z, Liu S, Lu N, Xu L, Shen Q, Huang Z, Huang Z, Saw PE, Xu X. Nucleus-specific RNAi nanoplatform for targeted regulation of nuclear LncRNA function and effective cancer therapy. Exploration. 2022;2:20220013.
49. Li S, Xu L, Wu G, Huang Z, Huang L, Zhang F, Wei C, Shen Q, Li R, Zhang L, Xu X. Remodeling Serine synthesis and metabolism via nanoparticles (NPs)-mediated CFL1 Silencing to enhance the sensitivity of hepatocellular carcinoma to Sorafenib. Adv Sci. 2023;10:2207118.
50. Xu X, Wu J, Liu S, Saw PE, Tao W, Li Y, Krygsman L, Yegnasubramanian S, De Marzo AM, Shi J, et al. Redox-responsive nanoparticle-mediated systemic RNAi for effective cancer therapy. Small. 2018;14:1802565.
51. Saw PE, Yao H, Lin C, Tao W, Farokhzad OC, Xu X. Stimuli-responsive polymer-prodrug hybrid nanoplatform for multistage SiRNA delivery and combination cancer therapy. Nano Lett. 2019;19:5967–74.
52. Xu X, Wu J, Liu Y, Saw PE, Tao W, Yu M, Zope H, Si M, Victorious A, Rasmussen J, et al. Multifunctional envelope-type SiRNA delivery nanoparticle platform for prostate cancer therapy. ACS Nano. 2017;11:2618–27.
53. Knop K, Hoogenboom R, Fischer D, Schubert US. Poly(ethylene glycol) in drug delivery: pros and cons as well as potential alternatives. Angew Chem Int Ed. 2010;49:6288–308.
54. Steeg PS. Tumor metastasis: mechanistic insights and clinical challenges. Nat Med. 2006;12:895–904.
55. Valastyan S, Weinberg Robert A. Tumor metastasis: molecular insights and evolving paradigms. Cell. 2011;147:275–92.
56. Lambert AW, Pattabiraman DR, Weinberg RA. Emerging biological principles of metastasis. Cell. 2017;168:670–91.
57. Ubellacker JM, Tasdogan A, Ramesh V, Shen B, Mitchell EC, Martin-Sandoval MS, Gu Z, McCormick ML, Durham AB, Spitz DR, et al. Lymph protects metastasizing melanoma cells from ferroptosis. Nature. 2020;585:113–8.

58. Xie Y, Wang B, Zhao Y, Tao Z, Wang Y, Chen G, Hu X. Mammary adipocytes protect triple-negative breast cancer cells from ferroptosis. J Hematol Oncol. 2022;15:72.
59. Rossi Sebastiano M, Pozzato C, Saliakoura M, Yang Z, Peng RW, Galie M, Oberson K, Simon HU, Karamitopoulou E, Konstantinidou G. ACSL3-PAI-1 signaling axis mediates tumor-stroma cross-talk promoting pancreatic cancer progression. Sci Adv. 2020;6:eabb9200.
60. Rossi Sebastiano M, Konstantinidou G. Targeting long chain acyl-CoA synthetases for cancer therapy. Int J Mol Sci. 2019;20:20153624.
61. Kulkarni JA, Witzigmann D, Thomson SB, Chen S, Leavitt BR, Cullis PR, van der Meel R. The current landscape of nucleic acid therapeutics. Nat Nanotechnol. 2021;16:630–43.
62. Paunovska K, Loughrey D, Dahlman JE. Drug delivery systems for RNA therapeutics. Nat Rev Genet. 2022;23:265–80.
63. Sasso JM, Ambrose BJB, Tenchov R, Datta RS, Basel MT, DeLong RK, Zhou QA. The progress and promise of RNA medicine-an arsenal of targeted treatments. J Med Chem. 2022;65:6975–7015.

Publisher's note